Search for double-Λ hypernuclei formation via $(\Xi^-, {}^{12}\mathrm{C})_{\mathrm{atom}} \rightarrow {}^{12}_{\Lambda\Lambda}\mathrm{B} + \mathrm{n}$

P. Khaustov[2], D. E. Alburger[1], P. D. Barnes[6], B. Bassalleck[12], A. R. Berdoz[2,*], A. Biglan[2,†], T. Bürger[9], D. S. Carman[2,‡], R. E. Chrien[1], C. A. Davis[11,7], H. Fischer[9], G. B. Franklin[2], J. Franz[9], L. Gan[11,§], A. Ichikawa[5], T. Iijima[3], K. Imai[5], Y. Kondo[5], P. Koran[2], M. Landry[11], L. Lee[11], J. Lowe[8,12], R. Magahiz[2,**], M. May[1], R. McCrady[2,††], C. A. Meyer[2], F. Merrill[6], S. A. Page[11], K. Paschke[2], P. H. Pile[1], B. Quinn[2], W. D. Ramsay[11], A. Rusek[1], R. Sawafta[1,‡‡], H. Schmitt[9], R. A. Schumacher[2], R. W. Stotzer[12,§§], R. Sutter[1], F. Takeutchi[4], W. T. H. van Oers[11], K. Yamamoto[5], M. Yosoi[5], V. J. Zeps[10]

(The AGS E885 Collaboration)

[1]*Brookhaven National Laboratory, Upton, NY 11973, USA*

[2]*Carnegie Mellon University, Pittsburgh, PA 15213, USA*

[3]*KEK, High Energy Accelerator Research Organization, Tsukuba, Ibaraki 305, Japan*

[4]*Kyoto Sangyo University, Kyoto 603, Japan*

[5]*Kyoto University, Sakyo-Ku, Kyoto 606, Japan*

---

*Present address: SFA Inc., Largo, MD 20774, USA

†Present address: Union Switch & Signal, Pittsburgh, PA 15219, USA

‡Present address: Ohio University, Athens, OH 45701, USA

§Present address: Hampton University, Hampton, VA 23668, USA

**Present address: Syncsort Inc., Woodcliff Lake, NJ 07675, USA

††Present address: Los Alamos National Laboratory, Los Alamos, NM 87545, USA

‡‡Present address: North Carolina A&T State University, Greensboro, NC 27411, USA

§§Present address: ASAP, Albuquerque, NM 87110, USA

[6]*Los Alamos National Laboratory, Los Alamos, NM 87545, USA*

[7]*TRIUMF, Vancouver, BC V6T 2A3, Canada*

[8]*University of Birmingham, Birmingham B15 2TT, UK*

[9]*University of Freiburg, D-79104 Freiburg, Germany*

[10]*University of Kentucky, Lexington, KY 40507 USA*

[11]*University of Manitoba, Winnipeg, Manitoba R3T 2N2, Canada*

[12]*University of New Mexico, Albuquerque, NM 87131, USA*

(December 23, 1999)

Abstract

Measurement of the energy of neutrons in coincidence with the production of free Ξ^- hyperons can be used to determine the masses of ${}^{12}_{\Lambda\Lambda}$B hypernuclear states and branching ratios of their formation from $(\Xi^-,{}^{12}\mathrm{C})_{\mathrm{atom}} \rightarrow {}^{12}_{\Lambda\Lambda}\mathrm{B} + \mathrm{n}$. The E885 collaboration utilized the Alternating Gradient Synchrotron (AGS) 1.8 GeV/c K^- beam incident on a diamond target to accumulate the largest-to-date data sample of $(\mathrm{K}^-,\mathrm{K}^+)$ events. A total of about 3×10^5 $(\mathrm{K}^-,\mathrm{K}^+)$ events have been collected and analyzed. The neutron spectrum shows no apparent peaks from the neutron-emission channel of double-Λ hypernuclear formation from $(\Xi^-,{}^{12}\mathrm{C})_{\mathrm{atom}}$ decay. The upper limit on the branching ratio of the above process has been set to be at or below 4% in the region of expected neutron energies.

Our understanding of the baryon-baryon interaction can be tested and expanded by studies of systems with non-zero strangeness. The YN interaction, in the $S = -1$ sector, has been explored by studies of Λ hypernuclei. However, unambiguous data pertaining to $S = -2$ systems are nearly nonexistent. Capture of Ξ^- hyperons on nuclei has been used as a technique in searches of double-Λ hypernuclei in emulsion based experiments. Measurements of the binding energies of double-Λ hypernuclei can be used to gain insight into the strength and sign of the $\Lambda\Lambda$ interaction. A total of three events, interpreted as double-Λ hypernuclear formation with reconstructed kinematics, have been reported over the past 36 years [1–3]. However, little is known for certain in the $S = -2$ sector, in part, because of the sparsity of data and, in part, due to the fact that emulsion events can have multiple interpretations. For example, alternative interpretations of the event reported in Ref. [3] result in opposite conclusions regarding the sign of the residual double-Λ interaction within a nucleus, $\Delta \mathrm{B}_{\Lambda\Lambda} = \mathrm{B}_{\Lambda\Lambda} - 2\,\mathrm{B}_{\Lambda}$. Here $B_{\Lambda\Lambda}$ refers to the total binding of the two Λs and B_{Λ} refers to the binding of a single Λ in a Λ-hypernucleus with the same nuclear core.

In E885, Ξ^- hyperons were produced from the reaction $\mathrm{K}^- +^{12}\mathrm{C} \rightarrow \mathrm{K}^+ + \mathrm{X} + \Xi^-$. Then Ξ^- capture at rest on carbon was used to attempt to produce double-Λ hypernuclei. A description of the experimental setup and event reconstruction has been reported in Ref. [4]. A fraction of the Ξ^-'s produced will stop before decaying and will then form $(\Xi^-,^{12}\mathrm{C})$ atoms. The subsequent Ξ^- atomic cascade could eventually result in the conversion $\Xi^- + \mathrm{p} \rightarrow \Lambda + \Lambda$. Atomic Ξ^- cascade calculations by C.J. Batty, quoted in ref [5], indicate that the capture occurs mainly from $3d$ and $4f$ atomic orbitals. The excess energy (Q = 28 MeV) in the conversion must be carried away via particle emission or fragmentation. One particularly interesting decay branch, from an experimental point of view, is the formation of a double-Λ hypernucleus accompanied by a mono-energetic neutron. The interpretation of the double-Λ emulsion event in the KEK-E176 experiment as $(\Xi^-,^{14}\mathrm{N})_{\mathrm{atom}} \rightarrow^{14}_{\Lambda\Lambda}\mathrm{C}^* + \mathrm{n} \rightarrow^{13}_{\Lambda\Lambda}\mathrm{B} + \mathrm{p} + \mathrm{n}$, which produces positive binding [6], hints at a significant neutron-emission channel for double-Λ hypernuclear formation. We note two calculations of neutron emission branching fractions. Zhu et al. [5] have predicted a branching fraction of around 3.4% for $(\Xi^-, {}^6\mathrm{Li})_{\mathrm{atom}} \rightarrow {}^{6}_{\Lambda\Lambda}\mathrm{He} + \mathrm{n}$. A recent calculation by T. Yamada and K. Ikeda predicts the branching ratio for $(\Xi^-, {}^{12}\mathrm{C})_{\mathrm{atom}} \rightarrow {}^{12}_{\Lambda\Lambda}\mathrm{B} + \mathrm{n}$, summed over all ${}^{12}_{\Lambda\Lambda}\mathrm{B}$ states, to be 1.48% [7]. For light nuclei, such as carbon, nitrogen, and oxygen; they estimate the two-Λ sticking probability to be around 5% for the combined production of double-Λ hypernuclei and pairs of single Λ hypernuclei per stopping Ξ^-. This is not inconsistent with the results of an emulsion experiment, KEK E176, which observed 3 such events for an estimated 30 Ξ^- stops in light nuclei [8] although the verification of the calculation is limited by the large experimental uncertainty.

In E885, a search for mono-energetic neutrons from the process $(\Xi^-, {}^{12}\mathrm{C})_{\mathrm{atom}} \rightarrow {}^{12}_{\Lambda\Lambda}\mathrm{B} + \mathrm{n}$ was performed to detect the formation of double-Λ hypernuclei. The final hypernuclear state generally could be excited, and there are several hypernuclear states that can be populated. Given a sufficient signal-to-noise ratio, the peak(s) could be reliably identified and measured. The number of events in a given peak and the corresponding neutron energy could then be used to determine both the branching ratio for the decay through neutron emission (for a particular hypernuclear state) and the energy of the hypernuclear state. For a measured neutron kinetic energy T_n, the mass of the double-Λ hypernucleus can be determined from energy conservation via the relation: $\mathrm{M}_{{}^{12}_{\Lambda\Lambda}\mathrm{B}} = \mathrm{M}_{(\Xi^-, {}^{12}\mathrm{C})_{\mathrm{atom}}} - \mathrm{M}_{\mathrm{n}} - \mathrm{T}_{\mathrm{n}}$, i.e. the energy of the hypernuclear state is the energy of the $(\Xi^-, {}^{12}\mathrm{C})$ atomic state minus the mass and kinetic energy of the emitted neutron (neglecting the recoil energy, which is much smaller than the detector resolution). From the neutron energy spectra of double-Λ hypernuclei, an important insight into the Λ-Λ interaction can be gained.

The experimental sensitivity to the production of double-Λ hypernuclei is directly proportional to the number of Ξ^- stops. Due to the short lifetime of the Ξ^-, most of the Ξ^-'s produced decayed before stopping. It is advantageous to use dense targets and higher beam intensities to maximize the production yield. These requirements preclude previous methods which relied on visual detection of the event, because emulsion or scintillator material have relatively low density and hence low stopping power, and a high flux would make the analysis difficult or impossible. The use of the high-intensity AGS D6 beam line and a high-density diamond target have allowed the accumulation of about 20,000 Ξ^- stops, which represents several orders of magnitude greater statistics than in all previous experiments.

The neutron detector arrays provided a large figure of merit (efficiency $\times$ stopping power $\approx 10\%$) [9] along with good timing resolution over a wide range of neutron energies. This was achieved by arranging 100 scintillator logs with dimensions 5.08 cm thick $\times$15.24 cm wide $\times$ 182.9 cm high in two stacks, one on each side of the target. Neutrons were detected through their elastic and inelastic interactions in the plastic scintillator (i.e. n-p and n-^{12}C interactions). Photomultipliers on both ends of each log provided the timing and amplitude of the signal from the neutron interaction. The mean-times of the signals for each log gave the neutron flight time from the target, and the time differences were used to determine the interaction coordinates along the extent of the log. The layer of veto counters placed in front of each set of neutron detectors was used to reject charged particles.

The initial velocity of the Ξ^- is strongly correlated with the missing mass of the reaction. The sensitivity to mono-energetic neutrons is maximized when events in the lower missing-mass region are selected, as this region corresponds to low Ξ^- initial velocity. The Ξ^- stopping probability, as a function of missing mass, was calculated in Monte Carlo simulation. The Ξ^- production was modeled as resulting from a collision of a K^- with an off mass-shell proton in the carbon nucleus. The proton momentum distribution was obtained using an harmonic oscillator model. The energy of the target proton was selected to conserve energy in the reaction. The angular distribution of the reaction was chosen to be flat in the K^--proton center-of-mass frame for small forward angles as observed for the elementary reaction [10]. Our model was found to reproduce the experimental missing-mass spectrum reasonably well. To determine the Ξ^- stopping probability, the Ξ^- was tracked until it either decayed or stopped. We note that the KEK E176 collaboration found that a similar model underestimated their measured fraction of Ξ^- stops in emulsion by 20 to 40% [11]. Therefore, it is possible that this model underestimates the stopping probability since it does not include Ξ^- final-state interactions that could yield a larger number of slow Ξ^-'s. We use the uncorrected Monte Carlo stopping probability estimates for a conservative calculation of the branching ratio upper limits.

Cuts applied to the missing-mass spectrum were selected to maximize the "quality factor" $Q = S/\sqrt{B}$ for the neutron spectrum. Here S represents the signal and $\sqrt{B}$ represents a measure of background fluctuation. Most of the detected neutrons came from π^- capture and other background processes, and these neutrons result in a smooth background spectrum. Any quantity proportional to signal or background can be used in the expression above for the purpose of selecting the cuts that maximize Q. The size of a peak in the neutron spectrum corresponding to hypernuclear production would be proportional to the product of the number of Ξ^- production events and the Ξ^- stopping probability. Therefore, the observed number of events times the estimated stopping probability was used for S. The shape of the neutron spectrum (excluding the γ peak at β=1) was determined to be independent of the $^{12}\mathrm{C}(\mathrm{K}^-,\mathrm{K}^+)\mathrm{X}$ missing-mass cut value. This, and the fact that any signal of double-Λ hypernuclear production would constitute a very small fraction of all events, led to the use of the number of entries in the neutron spectrum for B. Thus the expression for Q can be rewritten as $Q = \nu N/\sqrt{n}$, where ν, N, and n are the Ξ^- stopping probability, the number of events, and the number of entries in the neutron spectrum after the missing-mass cut, respectively. These are all functions of the missing-mass cut value. Using the stopping probability as predicted by Monte Carlo simulation, it was found that the missing-mass cut value of 11.637 GeV/c^2 maximizes Q, and this value was used to select events for the search of a mono-energetic neutron peak. For $^{12}\mathrm{C}(\mathrm{K}^-,\mathrm{K}^+)\mathrm{X}$ events with missing mass below 11.637 GeV/c^2, 31.7% of the Ξ^-'s were estimated to stop and form $(\Xi^-,^{12}\mathrm{C})$ atoms. A total of 54150 events survived the missing-mass cut. Extrapolating the background in the non-physical region of the missing-mass spectrum into the accepted region by assuming a flat background suggests that 1370 of the accepted events were background. The missing-mass spectrum is shown in Fig. 1 with the cut value shown by the arrow.

The neutron background shape was determined from the neutron spectrum of events with missing mass greater than 11.65 GeV/c^2, shown in Fig. 2a. The events are shown as a function of the inverse of the measured normalized neutron velocity, β = v/c, so that random accidental hits would appear as a flat background. The number of Ξ^- stops for the events in the higher missing-mass region is negligible and most neutrons in this data set are assumed to originate from the capture of Ξ^- decay-chain pions by nuclei. The neutron background spectrum was fit with a polynomial and the result, after appropriate scaling, was used as a background template for the neutron spectrum after the missing-mass cut. The neutron spectrum, after optimizing the missing-mass cut to maximize Q, is shown in Fig. 2b along with the scaled background template. It can be seen that the template shape provides a good description of the neutron spectrum for these events. Thus, the background in the neutron spectrum for the optimizing missing-mass cut is accounted for by using a scaled template of the neutron background obtained from the set of events which have a negligible Ξ^- stopping probability. (The neutron spectrum for β^{-1} from 1 to 3 shows a small dependence on the missing-mass cut. Similar effects have been seen in previous experiments involving stopping Ξ^- hyperons and are believed to be due, in part, to the stopping particles creating delayed nuclear γ-rays [12,13].)

For $(\Xi^-,{}^{12}\mathrm{C})_{\mathrm{atom}} \rightarrow{}^{12}_{\Lambda\Lambda}\mathrm{B} + \mathrm{n}$ the $(1\mathrm{s}_\Lambda 1\mathrm{p}_\Lambda)$ states are expected to be the most populated [5], with the nuclear core in the ground state or at low excitation energy. The binding energy of the ground state Λ in ${}^{11}_{\Lambda}\mathrm{B}$ is 10.24 MeV [14]. Taking the binding energy of the Λ in the $1p$ state to be 10 MeV less than the binding energy of the Λ in the ground state and assuming a ground state nuclear core gives, in the weak coupling limit,

$$\mathrm{M}_{{}^{12}_{\Lambda\Lambda}\mathrm{B}} = \mathrm{M}_{{}^{10}\mathrm{B}} + 2\mathrm{M}_\Lambda - 10.24\ \mathrm{MeV} - 0.24\ \mathrm{MeV} - \Delta\mathrm{B}_{\Lambda\Lambda}. \tag{1}$$

Neglecting recoil corrections and the binding energy of the Ξ^- in its atomic orbital, the kinetic energy of the neutron is

$$\mathrm{T}_\mathrm{n} = 11.3\ \mathrm{MeV} + \Delta\mathrm{B}_{\Lambda\Lambda}. \tag{2}$$

So the expected neutron energy is in the neighborhood of 11.3 MeV ($\beta^{-1} = 6.5$). Assuming a range between -4 MeV (repulsion) to 4 MeV (attraction) for $\Delta B_{\Lambda\Lambda}$, the neutron energy should be between 7.3 MeV and 15.3 MeV. Note that this $\Delta\mathrm{B}_{\Lambda\Lambda}$ is for the $(1\mathrm{s}_\Lambda 1\mathrm{p}_\Lambda)$ configuration and is different from the $\Delta\mathrm{B}_{\Lambda\Lambda}$ for the $(1\mathrm{s}_\Lambda 1\mathrm{s}_\Lambda)$ configuration found in emulsion experiments. There are indications from the emulsion experiments that the latter might be 4 MeV to 5 MeV, and the former is most likely considerably smaller due to the smaller overlap of the Λ wave functions. The neutron energy for the ground state production is $\mathrm{T_n} = 11.3$ MeV $+ 10$ MeV $+ \Delta\mathrm{B}_{\Lambda\Lambda}$ and is equal to 25.8 MeV for $\Delta\mathrm{B}_{\Lambda\Lambda} = 4.5$ MeV.

The expected width of the mono-energetic neutron peak is determined by the neutron detector energy resolution. The neutron detector energy resolution and efficiency were calculated in Monte Carlo simulation. It was found that the shape of the peak in the β^{-1} spectrum was close to being Gaussian for mono-energetic neutrons. For the nominal value of expected neutron kinetic energy, $\mathrm{T}_n = 11.3$ MeV ($\beta^{-1} = 6.5$), the neutron energy resolution was 0.16 units of β^{-1} (0.57 MeV). The neutron detection efficiency, calculated using the DEMONS code [9] was 6.1% at this energy. Our Monte Carlo prediction of the neutron energy resolution was found to agree with the measured energy resolution at a kinetic energy $\mathrm{T}_n = 18$ MeV, determined using neutrons from Σ^+ decays at rest. [12].

To find the number of mono-energetic neutrons for a particular neutron β^{-1}, the neutron spectrum was fit to the background template plus a Gaussian peak of the corresponding known width with the centroid at that value of β^{-1}. The background template scaling factor and Gaussian peak scaling factor were the two parameters of the fit. The number of events in the peak represents the best fit value for the number of mono-energetic neutrons from the neutron-emission channel of double-Λ hypernuclear formation. The corresponding 90% confidence level interval was then found using the ordering principle described by Feldman and Cousins [15]. The best fit value and the lower and upper boundaries of the confidence interval were then converted to branching ratios using $b = n/\epsilon(\beta^{-1})\nu N$, where N is the background-subtracted number of events (52780), $\epsilon(\beta^{-1})$ is the neutron detection efficiency corresponding to that β^{-1} (6.1% for $\beta^{-1} = 6.5$), and ν is the Ξ^- stopping probability (31.7%).

The fit procedure was repeated for a range of values of β^{-1} in order to obtain results as a function of β^{-1}. The results for the branching ratio are shown in Fig. 3. The dashed curve was found from the best fit value for the number of neutrons in a peak, and the shaded region is the 90% confidence band. The size of the interval is determined by the number of Ξ^- stops, the magnitude of the background and the best fit for the number of events in the hypothesized mono-energetic neutron peak found in the fit. The expected neutron energy given by Eq. 2, for $\Delta B_{\Lambda\Lambda} = 0$, is indicated by an arrow and the corresponding upper limit at this point is 3.3%. The difference between the nominal and the actual value of $B_{\Lambda\Lambda}$ determines the actual neutron energy. It is expected to be within ≈ 4 MeV from the central value and no signal is observed in this region. (The discrepancies with the background template near β^{-1}=3 lies outside the region of interest.) Our upper limits, which are below 4% over most the region corresponding to the expected neutron energy, do not contradict the T. Yamada and K. Ikeda prediction of a 1.48% neutron emission branching fraction spread over several states which lie in the continuum. [7].

This work is supported in part by the U. S. Department of Energy under contracts DE-FG02-91ER40609, DE-AC02-76H00016, and DE-FG03-94ER40821, by the German Federal Minister for Research and Technology (BMFT) under contract No. 06 FR 652, by the Natural Sciences and Engineering Research Council of Canada, and by the Japanese Society for the Promotion of Science.

REFERENCES

[1] M. Danysz *et al.*, Phys. Rev. Lett. **11**, 20 (1963).

[2] D. J. Prowse, Phys. Rev. Lett. **17**, 782 (1966).

[3] S. Aoki *et al.*, Prog. Theor. Phys. **95**, 1287 (1991).

[4] P. Khaustov *et al.*, Phys. Rev. C, submitted for publication (1999).

[5] D. Zhu, C. B. Dover, A. Gal, and M. May, Phys. Rev. Letters **67**, 2268 (1991).

[6] C. B. Dover,D. J. Millener, A. Gal, and D. H. Davis, Phys. Rev. C **44**,1905 (1991).

[7] T. Yamada and K. Ikeda, Phys. Rev. C **56**, 3216 (1997).

[8] K. Nakazawa, *Proc. of the 23rd INS International Symposium on Nuclear and Particle Physics with Meson Beams in the 1 GeV/c Region*, edited by S. Sugimoto and O. Hashimoto (Universal Academy Press, Tokyo, 1995), p. 261.

[9] R.C. Byrd *et al.*, Nucl. Instr. Meth. **A313**, 437 (1994); and B. Basselleck, private communication.

[10] C. Baltay *et al.*, Phys. Rev. D **9**, 49 (1974).

[11] K. Imai, private communication.

[12] F. Merrill, Ph.D. thesis, Carnegie Mellon University, (1995).

[13] L. Gan, Ph.D. thesis, University of Manitoba, (1998).

[14] M. Juric *et al.*, Nucl. Phys. **B52**, 1 (1973).

[15] G. J. Feldman and R. D. Cousins, Phys. Rev. D **57**, 3873 (1998).

FIGURES

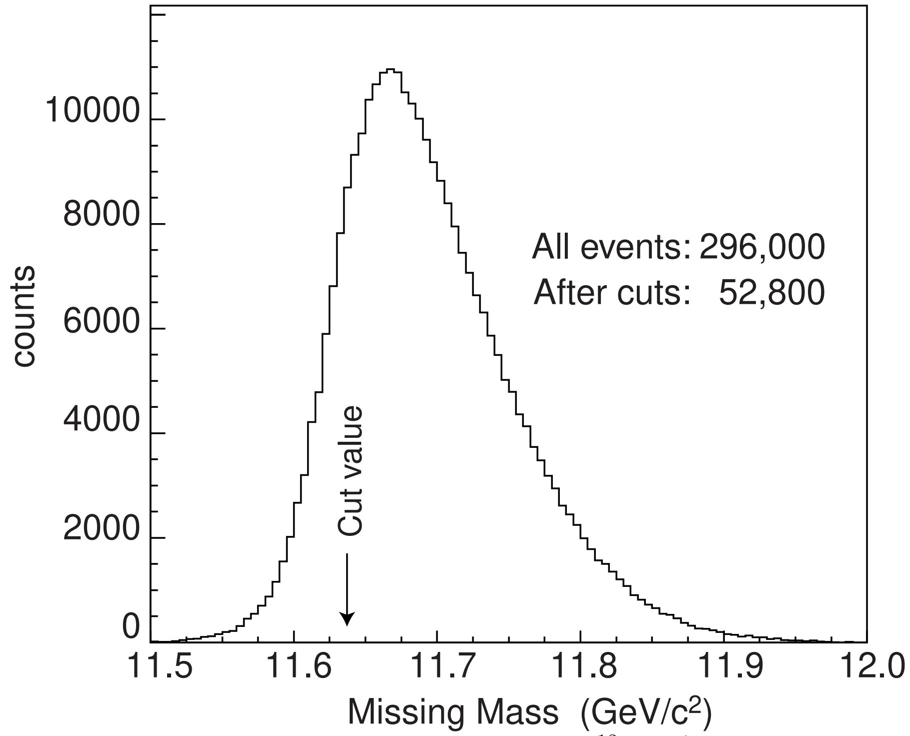

FIG. 1. Missing mass (background subtracted) for $K^-({}^{12}C, K^+)\Xi^-X$. Events whose missing mass is less than the cut value, indicated by the arrow, have a high Ξ^- probability of stopping in the diamond target and were used in this analysis.

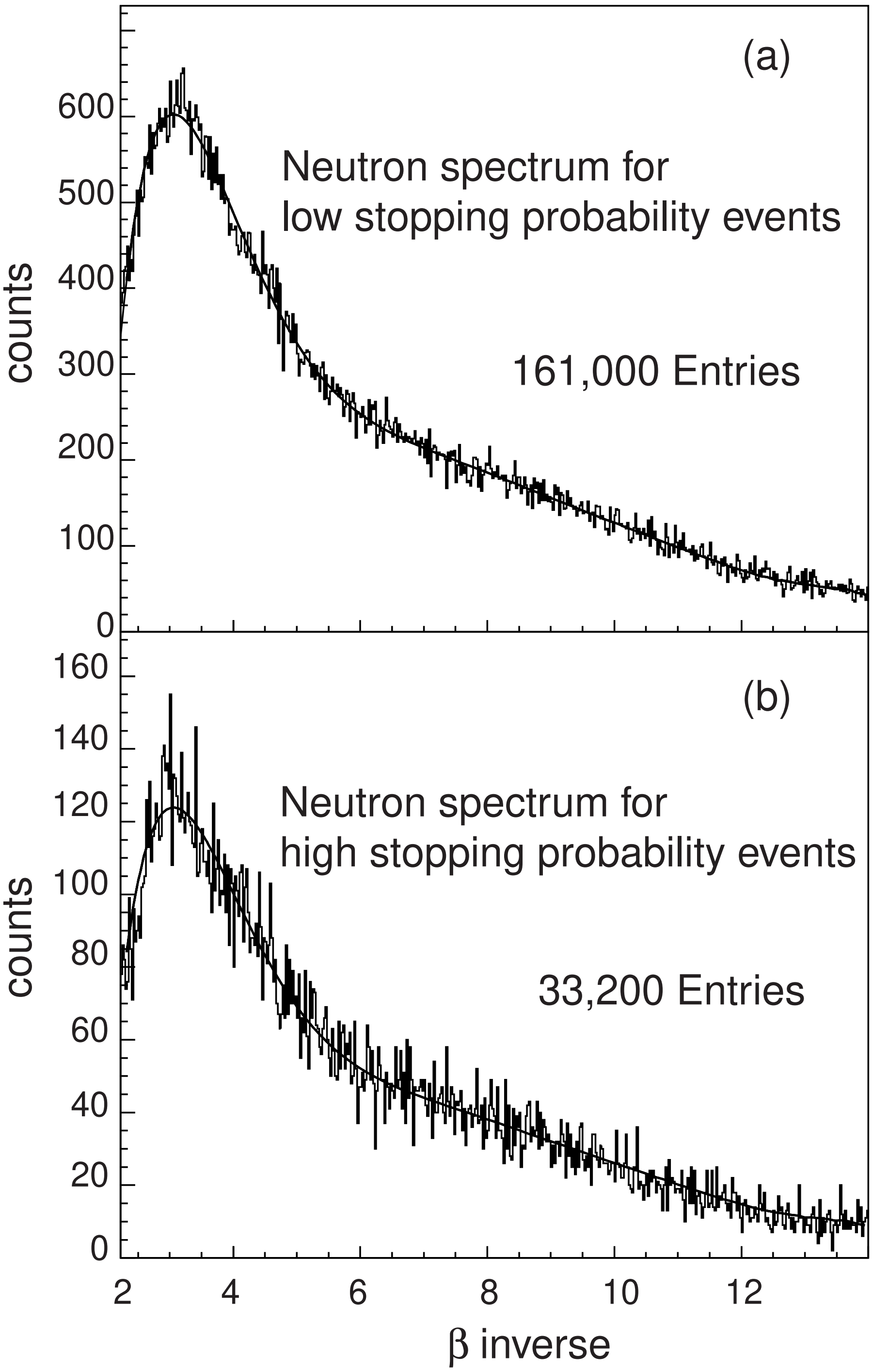

FIG. 2. (a) Neutron spectrum with de-optimized cuts (very low sensitivity) shown fitted with a polynomial which is used for the background template. (b) Neutron spectrum with optimized cuts (maximum sensitivity), shown with the scaled background template. The horizontal axis is $\beta^{-1} = c/v$.

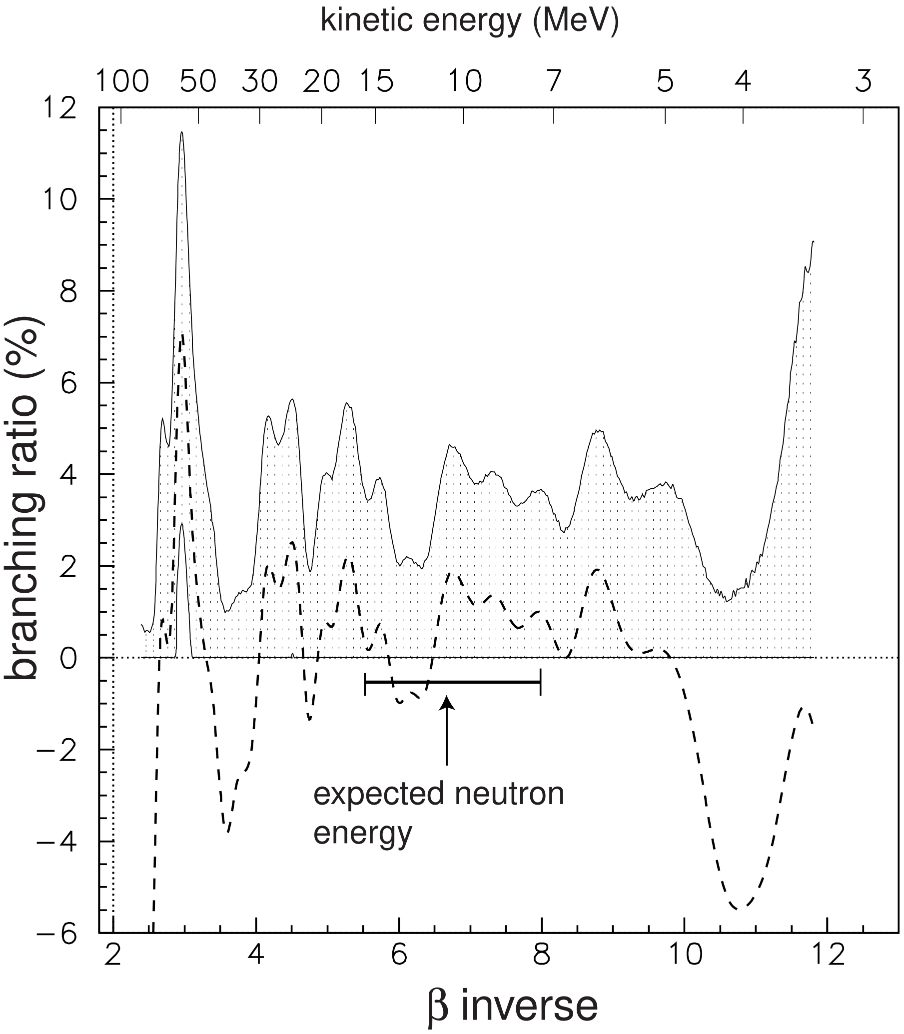

FIG. 3. The branching ratio for double-Λ hypernuclear formation via neutron emission $(\Xi^-, {}^{12}\mathrm{C})_{\mathrm{atom}} \rightarrow {}^{12}_{\Lambda\Lambda}\mathrm{B} + \mathrm{n}$ as a function of the neutron β^{-1}. The dashed curve shows the branching ratio obtained from the best fit value for the number of neutrons in the peak. The shaded band indicates the 90% confidence level interval for the branching ratio. The arrow indicates the expected neutron energy, with the assumptions described in the text. The bar shows the range of neutron β^{-1} which corresponds to -4 MeV $< \Delta\mathrm{B}_{\Lambda\Lambda} < +4$ MeV.